

The fabrication and characterization of poly(4-vinylpyridine)-based thin film transistors exhibiting enhanced ion modulation

Daniel Elkington, Darmawati Darwis, Xiaojing Zhou^{*}, Warwick Belcher, Paul C. Dastoor

Centre for Organic Electronics, University of Newcastle, Callaghan, NSW 2308, Australia

ARTICLE INFO

Article history:

Received 5 July 2011

Received in revised form 12 October 2011

Accepted 16 October 2011

Available online 7 November 2011

Keywords:

Organic thin film transistors

Ion diffusion

Ion drift

Electrostatic double layer

ABSTRACT

Lithium perchlorate-doped hygroscopic poly(4-vinylpyridine)-based organic thin film transistors have been fabricated and characterized. More than one mechanism of current modulation is observed in these devices with the observed mechanism depending upon both the amount of added dopant and the operating voltage. At low gate voltages (0 to -0.8 V) the current modulation mechanism is dominated by ions intrinsic to the dielectric layer (due to its hygroscopic nature), while at higher gate voltages (-1 to -2 V) the device behavior is governed by the movement of the dopant ions. Most importantly, through careful control of dopant concentration, we show that it is now possible to fabricate all-solution processed devices with significantly enhanced current modulation. In particular, we demonstrate that current modulation ratios in excess of 10^5 are possible with this device architecture.

© 2011 Elsevier B.V. All rights reserved.

1. Introduction

The development of organic thin film transistors (OTFTs) has grown rapidly in recent years, motivated primarily by the unique physical properties of polymer devices, including their flexibility and ability to be fabricated using low-cost solution-based techniques [1]. Conventional organic field-effect transistors (OFETs) typically require gate voltages (V_G) in the order of tens of volts in order to operate due to the limited charge carrier mobility of the conductive polymeric materials [2]. However, many applications for organic transistors require low voltage operation and, as such, much recent effort has been focussed on the development of OTFTs with lower operating voltages [3].

Low voltage OTFT operation often involves altering the properties of the dielectric layer, by increasing the specific capacitance of the material (by decreasing dielectric layer thickness or increasing the permittivity of the dielectric material) or changing the mechanism of device operation. One approach which has been introduced is utilizing

polymer electrolytes in which ions are added to induce a high charge density electrolyte double layer and thus enhanced drain currents (I_D) can be obtained in the order of several milliamps [4–6]. When these devices are operated in an inert environment, moisture-induced electrochemical doping can be avoided. When devices are characterized in air, both electrostatic double layer formation and electrochemical doping modulate the drain current at different operation gate voltages [7]. Another approach which has been reported involves using ion-conducting poly-electrolytes such as Nafion or poly(styrenesulfonic acid) (PSS:H) as the dielectric [8–10]. Although these types of devices can show good transistor characteristics, their off current (I_{OFF}) can be susceptible to increases at high relative humidity (RH) levels, making their performance variable under ambient conditions.

An early approach reported by Sandberg et al. uses poly(3-hexyl-thiophene) (P3HT)/poly(4-vinylphenol) (PVP)/poly(3,4-ethylenedioxythiophene):poly(styrene sulfonate) (PEDOT:PSS) as the semiconducting layer/dielectric layer/gate electrode, respectively [11–13]. The PVP dielectric is a highly hygroscopic material and moisture adsorbed by it plays a central role in modulating I_D under low V_G

^{*} Corresponding author. Tel.: +61 2 4921 6732; fax: +61 2 4921 6907.
E-mail address: xiaojing.zhou@newcastle.edu.au (X. Zhou).

values. The current modulation mechanism in these devices is chemical doping of the semiconducting channel stemming from ion diffusion at the dielectric-semiconductor interface [11]. These devices have maximum output currents (I_{ON}) of a few microamps, which is comparable to, or even higher than, many conventional OFETs. However, the current modulation ratios (I_{ON}/I_{OFF}) of hygroscopic insulator transistors depend highly on the RH level of where they are measured because of the large I_{OFF} associated with increased RH levels [8,14].

Devices of this type were fabricated in our laboratory and performed similarly to those reported by Sandberg et al. [13]. In these transistors, the combination of V_D and V_G controls the location of ions at the semiconductor/insulator interface layer. For a given negative V_G , anions migrate to this interface and induce an increase in conductance in the P3HT layer. The effect on I_D of increasing V_D is balanced by an increased fraction of low conductance P3HT in the channel (induced by the movement of ions along the interface) which leads to a saturation of I_D , effectively resembling a conventional field-effect transistor mechanism. I_{ON}/I_{OFF} ratios of between 10 and 100 were observed – this lower than expected value can be attributed to a high relative humidity causing an increase in I_{OFF} (the RH has been consistently recorded as $50 \pm 10\%$ in the laboratory in which these devices were characterized). Another possible cause of high I_{OFF} in these devices is the contribution of the acidic PEDOT:PSS suspension which is drop-cast as a gate electrode [15]. Protons from the PEDOT:PSS likely diffuse across the PVP layer and further dope the P3HT layer.

A key challenge then, is to improve the low current modulation ratio that results from the high I_{OFF} at a relative high humid environment. In this paper, we show that by changing the hygroscopic polymer and subsequently doping the dielectric layer we are able to fabricate OTFT devices with greatly reduced I_{OFF} and significantly enhanced current modulation. Furthermore, we show that at low V_G the current modulation mechanism is dominated by the movement of ions associated with the hygroscopic nature of the dielectric whereas at high V_G it is governed by the movement and diffusion of the dopant ions. Consequently, we demonstrate that by using lithium perchlorate (LiClO_4)-doped poly(4-vinylpyridine) (PVPy) as the dielectric, an all solution-processible, low operating voltage transistor can be fabricated with greatly enhanced transistor performance parameters.

2. Material and methods

All devices were fabricated on glass substrates with pre-patterned indium-tin-oxide (ITO) source and drain electrodes. The channel length and width is $20 \mu\text{m}$ and 3mm , respectively. P3HT was purchased from Rieke Metals and dissolved in chloroform at a concentration of 20mg/mL . A 100nm thick P3HT layer was spin-coated (60s at 2000rpm) onto the substrate as measured by a KLA Tencor profilometer. Dielectric materials PVP and PVPy (Aldrich) and dissolved in ethanol at a concentration of 80mg/mL . LiClO_4 (Aldrich) was dissolved in the PVPy solution in various concentrations. The dielectric layers were spin-coated (60s

at 2000rpm) to a thickness of approximately 500nm . The P3HT/PVP or P3HT/PVPy two-layer structures were annealed at 85°C in air to remove any remaining solvents. Lastly, PEDOT:PSS (Aldrich, pH 1–2) was drop-cast on the top of gate dielectric layer and dried on a hot plate at 40°C in air. Two Keithley 2400 source meters were used for the device characterization. All output characteristic measurements have been conducted at a scan rate 0.1V/s . All fabricated devices were measured in air immediately after drying the PEDOT:PSS layer. The RH has been consistently recorded as $50 \pm 10\%$ in the laboratory in which these devices were characterized.

3. Results and discussion

One approach for reducing the inherently high I_{OFF} in PVP-based OTFTs is to decrease the number of mobile protons in the dielectric layer by replacing the acidic PVP with a hygroscopic polymer which is basic in nature. PVPy is another polyvinyl aromatic polymer where the phenol group has been replaced by a pyridine moiety. As shown in Fig. 1, whereas PVP is weakly acidic (and therefore acts as a proton source), PVPy is weakly basic and acts as a proton acceptor [16]. Fig. 2 shows the difference in I_{OFF} and I_G in the off state for PVP- and PVPy-based devices. There is a clear reduction in I_{OFF} in the PVPy case indicating that the attempt to reduce the inherent doping level of the P3HT layer has been successful, and that this can be attributed to the PVPy being more effective in blocking current contributions from the gate and/or doping of P3HT due to diffusion of protons from the PEDOT:PSS suspension.

Fig. 3(a) shows the output characteristics of a transistor employing PVPy as the dielectric layer. Again, FET-like drain current modulation is exhibited and the output characteristic is very similar to that of the PVP-based device. However, the I_D measured for PVPy-based transistors are generally one order of magnitude lower than those for the corresponding PVP-based devices confirming that there are fewer mobile protons. Nevertheless, the current modulation ratio of the PVPy-based transistors is between 10 and 100, as shown in Fig. 3(b), which is comparable to that observed for the PVP-based devices at a high humidity level. This close agreement in results implies that the benefits of reducing I_{OFF} have been largely offset by an associated reduction in I_{ON} . Fig. 3(b) shows that the transfer characteristic of the PVPy-based device is highly reversible

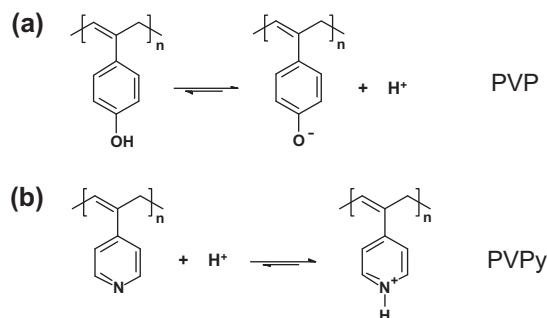


Fig. 1. The molecular structure of (a) PVP and (b) PVPy.

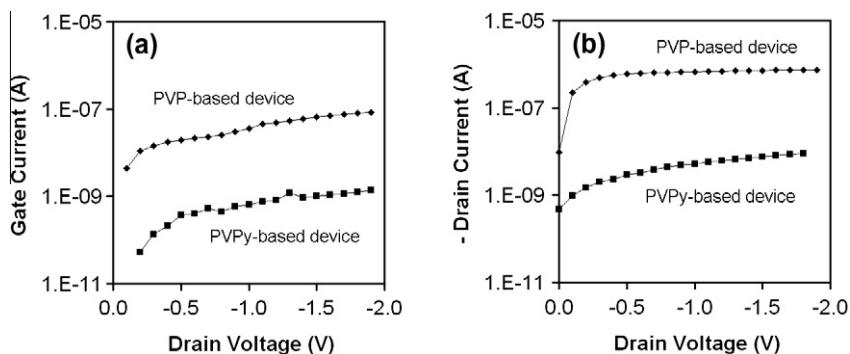


Fig. 2. Comparison of I_G and I_D in PVP and PVPy-based devices at $V_G = 0$ V. (a) I_G and (b) $-I_D$.

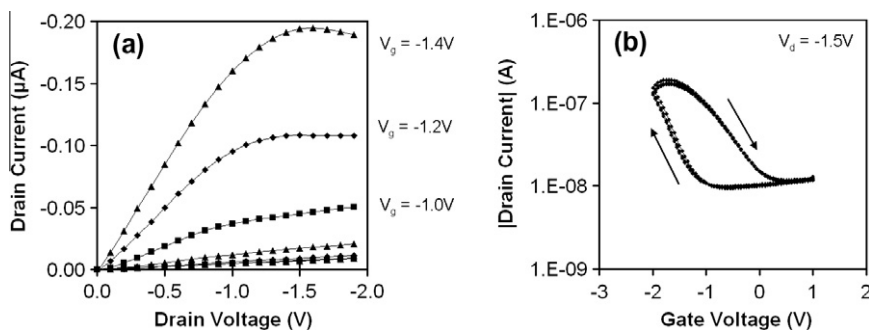


Fig. 3. Current–voltage characteristics of a PVPy-based OTFT. (a) Output characteristic for V_G from 0 to -1.0 V in -0.2 V steps and (b) transfer characteristic at $V_D = -1.5$ V, V_G scan rate = 50 mV/s. Three cycles from $V_G = 1$ to -2 V.

and reproducible, although there is a large amount of hysteresis between the forward and the reverse V_G scan directions, with the threshold voltage being shifted towards positive values in the reverse scan direction. This hysteresis could be indicative of a rough interface between P3HT/PVPy and PVPy/PEDOT, whereby the ions which have been attracted to the interfaces of the PVPy are less inclined to relax or be induced back into the bulk of the layer dielectric layer upon a change in V_G .

The mechanism of operation of the PVPy-based devices appears to be similar to that of the PVP-based devices, except that now we postulate that a significant fraction of the protons are immobilised as pyridinium cations. Consequently, dopant anions (such as hydroxyls) are removed from the channel interface and immobilised within the dielectric as pyridinium salts. As such, the P3HT channel maintains its low intrinsic conductivity as opposed to the doped state of the PVP-based devices.

Thus, further improvement in device performance requires maintaining a relatively low I_{OFF} whilst improving I_{ON} substantially. One approach is to introduce an ionic species into the dielectric which would enhance current modulation beyond a certain threshold value of V_G without increasing I_{OFF} . Figs. 4–6 show the electrical characteristics of PVPy transistors with various concentrations of $LiClO_4$ added to the PVPy solution. Fig. 4(a) and (b) shows the output characteristics for a device with $LiClO_4$ added to a concentration of 0.005 M, for -0.8 V $\leq V_G \leq 0$ V and -2 V $\leq V_G \leq 0$ V, respectively. The output characteristics are

similar to an undoped PVPy device for -0.8 V $\leq V_G \leq 0$ V, whilst for more negative values of V_G there is no increase in I_D and gate leakage current starts to dominate the device's behavior. Fig. 5(a) and (b) shows the output characteristics for a device with a $LiClO_4$ concentration of 0.02 M for the same V_G conditions. In this case, we see evidence for the emergence of a second current modulation regime: for -0.8 V $\leq V_G \leq 0$ V, 'normal' operation for a PVPy-based device is observed whereas for $V_G \leq -1.2$ V, the current modulation exhibits enhanced drain currents but no saturation of I_D is obtained at V_D less than -2.0 V. As such, we propose that for $V_G \leq -1.2$ V the $LiClO_4$ starts to contribute to device performance and the current modulation begins to be influenced by the movement and diffusion of the introduced ions. Although the leakage current becomes quite significant at this concentration of $LiClO_4$ for $V_G \leq -1.2$ V (since relatively large positive I_D is observed at $V_D \approx 0$ V), Fig. 5(b) is designed to show the onset of a new mechanism which influences the device's electrical characteristics.

In Fig. 6(a) and (b), the output characteristics for the same V_G ranges are shown for $LiClO_4$ in the PVPy solution at a concentration of 0.2 M. The results show that there are now two clearly defined voltage regimes for the operation of these thin film transistors. Again, for -0.8 V $\leq V_G \leq 0$ V, 'normal' operation for a PVPy-based device is observed whereas for $V_G \leq -1.2$ V, the current modulation is dominated by much larger drain currents that saturate at $V_D \approx -2.0$ V. Most importantly, while I_{OFF} in this device is comparable to the PVPy only device, I_{ON} is now in the

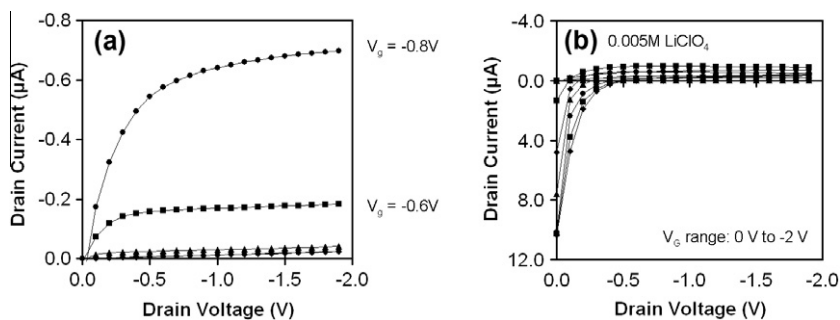


Fig. 4. The effect of 0.005 M LiClO₄ concentration on the performance of a PVPy-based device for V_G in the range (a) 0 to -0.8 V and (b) 0 to -2.0 V.

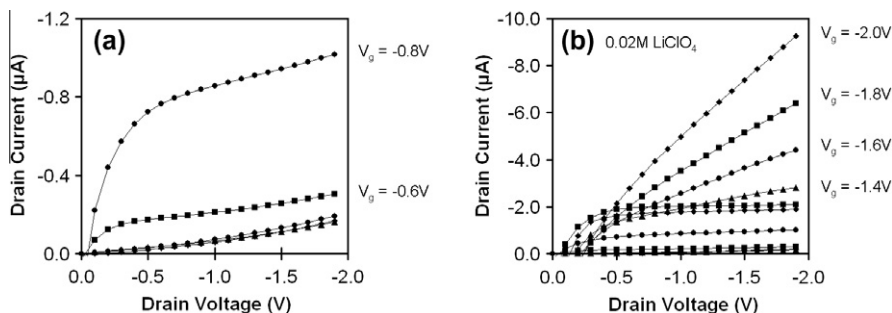


Fig. 5. The effect of 0.02 M LiClO₄ concentration on the performance of a PVPy-based device for V_G in the range (a) 0 to -0.8 V and (b) 0 to -2.0 V.

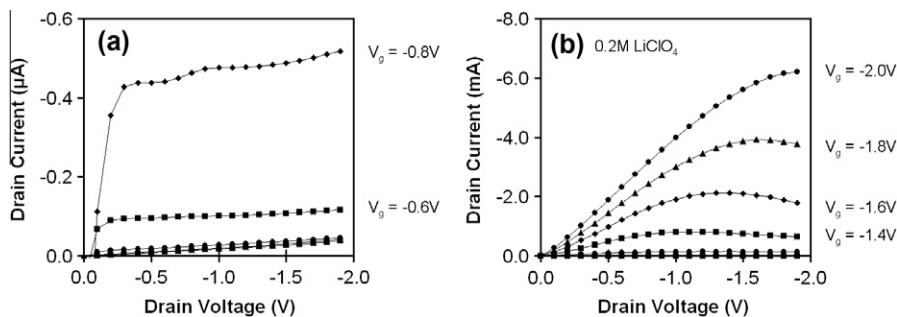


Fig. 6. The effect of 0.2 M LiClO₄ concentration on the performance of a PVPy-based device for V_G in the range (a) 0 to -0.8 V and (b) 0 to -2.0 V.

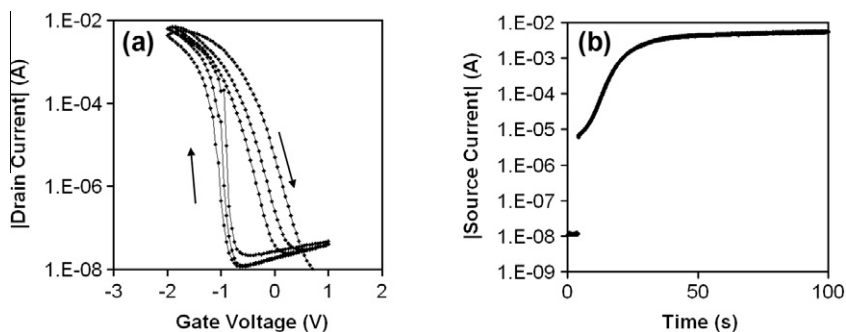


Fig. 7. (a) Transfer characteristic of PVPy:LiClO₄(0.2 M) device. V_D = -1.5 V. V_G scan rate = 0.5 mV/s (50 mV/100 s). (b) Switch-on characteristic for a PVPy:LiClO₄(0.2 M)-based device (sampling frequency of 100 Hz). V_G = from 0 to -2 V, V_D = -2 V.

milliamp range and the current modulation ratio of these devices reaches a value in the order of 10^5 ; several orders of magnitude higher than both the PVP- and PVPy-based devices.

Similarly, large I_{ON}/I_{OFF} values have been reported for OTFT devices based on a variety of polymer electrolyte dielectrics [4,5,10,17]. For example, using polyethylene oxide doped with LiClO_4 as the gate dielectric, Frisbie and co-workers showed that current modulation ratios of 10^4 and 10^5 could be achieved for pentacene [18] and single crystal rubrene [6], respectively. In these devices, the application of a negative V_G drives cations to the gate and anions to the active layer interface but creates an electrostatic Helmholtz double layer across the dielectric rather than doping the active layer. These electrical double layer capacitor (EDLC) devices are characterized by their low voltage operation (<1 V), high specific capacitances (as high as $500 \mu\text{F cm}^{-2}$) and high I_{ON}/I_{OFF} (up to 10^5) [8].

Whilst the specific (per area) capacitance of OTFTs is often estimated using the equation for saturation current in a field-effect device ($I_{D,sat} = (W/2L) \mu C_i (V_G - V_T)^2$, where W and L are the channel width and length, respectively, μ is the semiconductor charge carrier mobility, C_i is the specific capacitance of the dielectric layer and V_T is the threshold voltage), the values obtained for the plain PVPy and 0.2 M LiClO_4 -doped PVPy are $1.7 \mu\text{F/cm}^2$ and 5.6mF/cm^2 , respectively, both of which are several orders of magnitude higher than values obtained by directly measuring the capacitance with a capacitance meter (for further details on these calculations see the Supporting Information). This observation supports our postulate that the mechanism of these devices is electrochemical nature and does not involve a conventional field effect.

Fig. 7(a) shows the transfer curve of a $\text{LiClO}_4(0.2 \text{ M})$ -doped PVPy device at $V_D = -1.5$ V, clearly showing reversible and repeatable performance, with a current modulation ratio of over 10^5 . Despite a low scan rate of 0.5 mV/s , a high level of hysteresis in the repeated scans is observed indicating that a slow ionic process dominates the device performance. This observation is consistent with the ion concentration dependant current modulation shown in Figs. 4–6. For the 0.2 M LiClO_4 device, I_{ON} is in the order of milliamps, which is three orders of magnitude larger than I_G in the on state (as shown in Supporting Information Fig. 2). If I_G is solely from ionic conductance in the PVPy layer then the much larger I_D is most likely due to an electrochemical doping process which induces a high electronic conductance in the active layer when the device is switched on.

Time dependent current measurements can be used to distinguish between the possible mechanisms operating in LiClO_4 doped PVPy devices [10]. Fig. 7(b) shows the source current (I_S) response of the PVPy: $\text{LiClO}_4(0.2 \text{ M})$ -based device to a single step in V_G from 0 to -2 V, with V_D held at -2 V. Initially, a fast step change in current is observed with a magnitude of between 1 and $10 \mu\text{A}$. Subsequently, there is a slow rise in current until a maximum current value in the milliamp range (coinciding with the expected value from Fig. 6(b)) is achieved after about 100 s. Clearly, the mechanism of this slow rise cannot be due to the formation of an electrical double layer, which

occurs on a much shorter time scale [19]. Furthermore, the large currents are not due to gate leakage since I_G has been observed to be several orders of magnitude lower under these conditions when output characteristics have been measured (see Supporting Information Fig. 2). Therefore, we postulate that the fast initial change in current, which occurs within 10 ms of V_G switching, is most likely due to electrical double layer formation, while the subsequent slow increase in current is due to a diffusion-based electrochemical doping of the semiconductor channel.

Compared to conventional OFETs where operation frequencies are generally a concern, hygroscopic dielectric based OTFTs can achieve air-compatible, printable, reliable, low voltage operation and high current amplification. This type of OTFTs can find applications in chemical and biosensing where high operation frequencies are not required [20,21]. Ion-doped PVPy-based OTFTs appear to be good candidates to satisfy these criteria.

4. Conclusions

Two hygroscopic dielectric materials, PVP and PVPy, have been implemented to fabricate solution processible organic thin film transistors. Transistors with either dielectric layer can be operated at $|V_G| < 1$ V. Transistors with a PVP dielectric layer exhibit intrinsic anionic doping of the P3HT channel which induces a significant on-current even without an applied V_G . By contrast, transistors with a PVPy dielectric layer immobilise a significant fraction of the mobile anions resulting in less doping of the P3HT channel and substantially lower I_{ON} and I_{OFF} . Subsequent addition of LiClO_4 results in a less mobile anion dopant and the creation of a second current modulation regime. With this dopant, at $V_G < -1.2$ V electrochemical doping of the P3HT channel results in low I_{OFF} , high I_{ON} and an associated significant increase in current modulation.

Acknowledgements

The University of Newcastle is gratefully acknowledged for PhD scholarships (DE). We acknowledge financial support from the Commonwealth of Australian Research Council through Discovery Project Funding Scheme.

Appendix A. Supplementary data

Supplementary data associated with this article can be found, in the online version, at doi:10.1016/j.orgel.2011.10.014.

References

- [1] H. Sirringhaus, Adv. Mater. 17 (20) (2005) 2411–2425.
- [2] A. Facchetti, M.H. Yoon, T.J. Marks, Adv. Mater. 17 (14) (2005) 1705–1725.
- [3] B.N. Pal, B.M. Dhar, K.C. See, H.E. Katz, Nat. Mater. 8 (11) (2009) 898–903.
- [4] M.J. Panzer, C.D. Frisbie, J. Am. Chem. Soc. 127 (19) (2005) 6960–6961.
- [5] M.J. Panzer, C.D. Frisbie, J. Am. Chem. Soc. 129 (20) (2007) 6599–6607.
- [6] M.J. Panzer, C.D. Frisbie, Appl. Phys. Lett. 88 (20) (2006) 203504-1–203504-3.

- [7] J.D. Yuen, A.S. Dhoot, E.B. Namdas, N.E. Coates, M. Heeney, I. McCulloch, D. Moses, A.J. Heeger, *J. Am. Chem. Soc.* 129 (46) (2007) 14367–14371.
- [8] O. Larsson, E. Said, M. Berggren, X. Crispin, *Adv. Funct. Mater.* 19 (20) (2009) 3334–3341.
- [9] N.J. Kaihovirta, C.J. Wikman, T. Mäkelä, C.E. Wilén, R. Österbacka, *Adv. Mater.* 21 (24) (2009) 2520–2523.
- [10] L. Herlogsson, X. Crispin, N.D. Robinson, M. Sandberg, O.J. Hagel, G. Gustafsson, M. Berggren, *Adv. Mater.* 19 (1) (2007) 97–101.
- [11] T.G. Bäcklund, H.G.O. Sandberg, R. Österbacka, H. Stubb, *Appl. Phys. Lett.* 85 (2004) 3887.
- [12] H.G.O. Sandberg, T.G. Bäcklund, R. Österbacka, S. Jussila, T. Makela, H. Stubb, *Synt. Met.* 155 (3) (2005) 662–665.
- [13] H.G.O. Sandberg, T.G. Bäcklund, R. Österbacka, H. Stubb, *Adv. Mater.* 16 (13) (2004) 1112–1115.
- [14] E. Said, O. Larsson, M. Berggren, X. Crispin, *Adv. Funct. Mater.* 18 (21) (2008) 3529–3536.
- [15] M.P. De Jong, L.J. Van Ijzendoorn, M.J.A. De Voigt, *Appl. Phys. Lett.* 77 (2000) 2255.
- [16] J.L. Velada, L.C. Cesteros, E. Meaurio, I. Katime, *Polymer* 36 (14) (1995) 2765–2772.
- [17] M.J. Panzer, C.D. Frisbie, *Adv. Funct. Mater.* 16 (8) (2006) 1051–1056.
- [18] M.J. Panzer, C.R. Newman, C.D. Frisbie, *Appl. Phys. Lett.* 86 (2005) 103503.
- [19] J. Wang, *Analytical Electrochemistry*, Wiley-VCH, 2000.
- [20] D.J. Macaya, M. Nikolou, S. Takamatsu, J.T. Mabeck, R.M. Owens, G.G. Malliaras, *Sens. Actuators, B: Chem.* 123 (1) (2007) 374–378.
- [21] S.K. Kanakamedala, H.T. Alshakhouri, M. Agarwal, M.A. DeCoster, *Sens. Actuators, B: Chem.* 157 (1) (2011) 92–97.